

Petromagnetism of Ores and Host Rocks in the Southern Omolon Ore District (Northeast Russia)

Yu. Yu. Ivanov, P. S. Minyuk, N. I. Tret'yakova, E. V. Kolesov, and M. I. Fomina

*Shilo Northeast Complex Research Institute, Far East Branch, Russian Academy of Sciences,
ul. Portovaya 16, Magadan, 685000 Russia*

e-mail: pal105@neisri.ru

Received April 12, 2014

Abstract—The petromagnetic properties of rocks from the Verkhniy Omolon, Magnetitovyi, Innyaga, and Alekseevskii areas of the Southern Omolon iron-ore district located in the southern part of the Omolon Massif (Northeast Russia) are investigated. The maximum values of natural remanent magnetization (NRM) and magnetic susceptibility (k) of 22.8–1196 A/m and 1046×10^{-3} SI on average, respectively, are typical of ferruginous quartzite from the Innyaga site. The amphibolites exhibit high values of these magnetic parameters: J_n is approximately 28.6 A/m and k is 45×10^{-3} SI. The magnetic properties (J_n and k) of the plagiogneisses and granite gneisses are highly heterogeneous and variable. The migmatites, rhyolites, and dacites are submagnetic. Magnetic minerals are largely represented by multidomain and pseudosingle-domain magnetites and their oxidation products such as maghemite, hematite, and iron hydroxides. It is revealed that the amphibolites are characterized by normal polarity of the remanent magnetization, while the ferruginous quartzites demonstrate normal and reverse polarities. These rocks may serve as sources of magnetic bipolar anomalies.

Keywords: ferruginous quartzite, magnetic properties, Omolon Massif, Northeast Russia

DOI: 10.1134/S181971401504003X

INTRODUCTION

Special complex geological–geophysical studies in the southern Omolon Massif have revealed several lodes of ferruginous quartzites, which provided grounds for distinguishing the Omolon iron-ore province, with the Southern Omolon iron-ore district being its most promising area [5]. This region hosts more than ten iron-ore occurrences [25]. Ferruginous quartzites are represented by lens-shaped and stratiform bodies among migmatites, amphibole and biotite–amphibole plagiogneisses, amphibolites, and basic crystalline schists. No uniform viewpoint exists on the genesis and age of ferruginous quartzites. Most researchers consider them as being metasomatic rocks [14] related to Early Proterozoic granitization. Some authors [9] accept the metasomatic nature of ferruginous quartzites, assuming, however, a two-stage process with the formation of ores during Riphean destruction of the crystalline basement. Other researchers suggest a sedimentary origin of iron ores [7]. For prospecting and exploring magnetite ores, geophysical methods including ground and aeromagnetic surveying are widely used [11]. Correct interpretation of the data obtained by magnetic surveying requires knowledge of the magnetic properties of rocks. Despite the fact that iron-ore mineralization in the Omolon Massif has been known for a long time,

the magnetic properties of its rocks remain insufficiently studied. The study of the magnetic properties of the rocks in the region in question is aimed at the assessment of the share of inductive and natural remanent magnetization in the intensity of the magnetic anomalies revealed by the ground magnetometric survey, which is of importance for contouring ore bodies [10].

MATERIALS AND METHODS

The petromagnetic properties of rocks were studied in a total of 120 samples from the Verkhniy Omolon, Magnetitovyi, Innyaga, and Alekseevskii areas of the South Omolon iron-ore district located in the southern part of the Omolon Massif (Fig. 1). For study, oriented and nonoriented samples taken from outcrops and boreholes were used.

Natural remanent magnetization (J_n , NRM) was measured at the JR-5A (AGICO Ltd.) spin magnetometer. Prior to assessing the stability, the samples were held for 5–15 days in the “along the field” and “opposite to the field” states to be demagnetized by the variable field with amplitudes of 5, 10, 20, 40, and 60 mT on LDA-3 (AGICO Ltd.) equipment. The Remasoft program was used for calculating the obtained data.

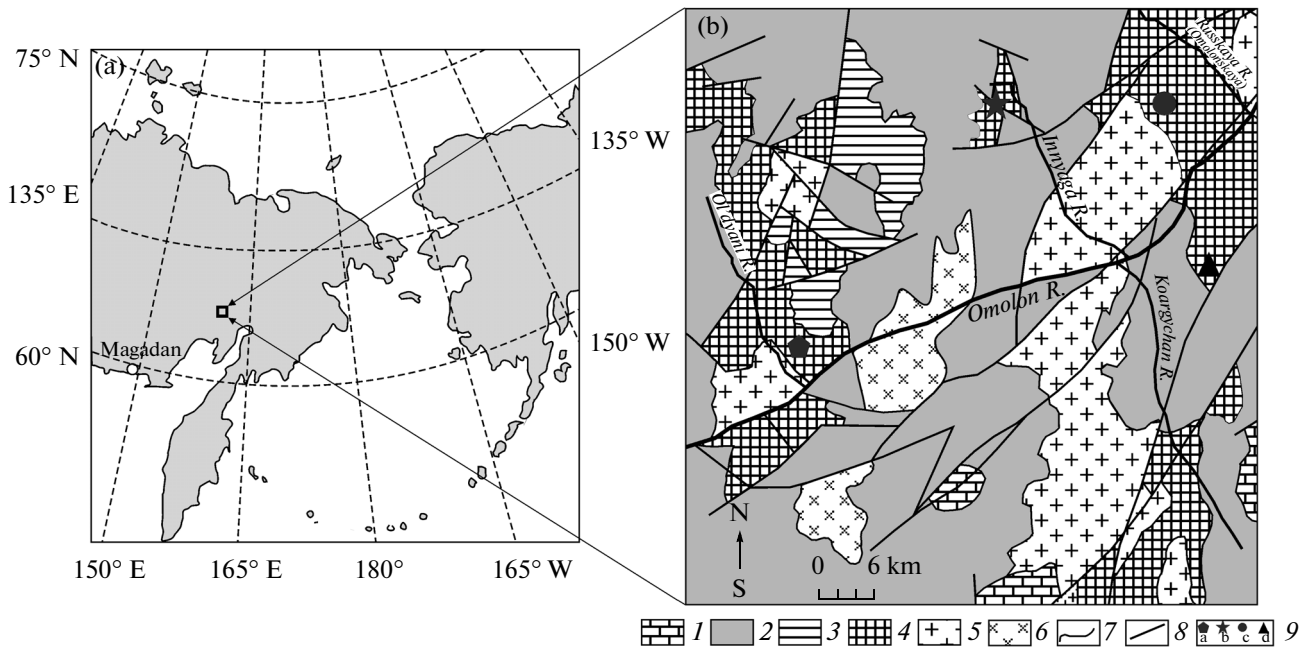


Fig. 1. Location (a) and schematic geological map of the South Omolon iron-ore district (b) (after [6] modified).
 (1) sedimentary rocks (P_1-K_2); (2) volcanogenic rocks of the Kedon Complex (D_{2-3kd}); (3) Riphean sedimentary rocks (PR_2); (4) pre-Riphean crystalline basement; (5) Early Paleozoic intrusive rocks; (6) Middle Paleozoic granitoids; (7) geological boundaries; (8) tectonic fractures; (9) sampling areas: (a) Verkhniy Omolon, (b) Innyaga, (c) Magnetitovyi, (d) Alekseevskii.

The magnetic susceptibility (MS, k) and temperature dependence of k in the temperature interval of 20–700°C in the air and argon mediums were measured on an MFK1-FA multifunctional kappameter with the CS-3 (AGICO Ltd.) thermal attachment. The heating and cooling rates were approximately 12–13°C/min and the maximum heating temperature was 700°C. Some samples were heated in the argon medium. The parameters of magnetic hysteresis, including remanent saturation magnetization (J_{rs}), saturation magnetization (J_s), inductive magnetization (J_i), coercive force (B_c), and remanent coercive force (B_{cr}) were measured on a J -meter automatic coercimeter [2]. The maximum value of the induced field was up to 500 mT. The relative share of the paramagnetic component was calculated using the formula $[J_i \text{ (at 500 mT)} - J_s \text{ (ferromagnetic component)}] / J_i \text{ (at 500 mT)}$. For analyzing the dependence of saturation magnetization on temperature $J_s(T)$, magnetic scales were used in an induction field of 500 mT [2]. The samples were heated to 700°C with the heating rate of approximately 100°C/min. The rock density was measured on an IMT-3 densitometer.

The mineralogical composition of the rocks was studied with a MT 9000 Series polarization microscope. Some samples were examined on Qemscan equipment (Australia), which includes an EVO-50 scanning microscope and Quantax Espirit (Bruker) energy dispersion system.

BRIEF REVIEW OF AREAS

Systematic geological studies in the Omolon Massif were started in the 1930s and continue to the present.

In the 1970s, special and complex geological–geophysical studies in the southwestern part of the Omolon Massif revealed several large iron-ore occurrences. This discovery provided grounds for defining the South Omolon iron-ore district in this region.

The evaluation survey carried out by geologists of the Northeast Regional Geological Agency (L.G. Shpil’ko and A.P. Fadeev, 1973) with the aim of revealing iron-ore objects in this area was accompanied by the analysis of different regional aspects of its stratigraphy, magmatism, tectonics, and mineral resources with generalization of the data on the physical and petrochemical properties of rocks and interpretation of the anomalous magnetic field [5, 7, 14].

The new data on the geological structure of the region under consideration were obtained during prospecting works carried out by the Dukat Mining–Geological Company in 2009–2012 [13].

The Upper Omolon area is located on the left side of the Ol’dyani River in its lower reaches (Fig. 1). The central part of the ore field, approximately 8 km² in size and composed of migmatites, gneisses, and amphibolites, comprises five ore lodes dipping mostly in the easterly to northeasterly directions. The lodes are formed by conformable subparallel lens-shaped bodies of ferruginous quartzites up to 160 m thick and

1100 m long. The vertical section of mineralization varies from 300 to 500 m in thickness. The ores include the following minerals: magnetite (35–50%); quartz (15–50%); amphibole (up to 10%), and accessories represented by apatite, ilmenite, and zircon. The ores are characterized by lenticular–banded structures, densely disseminated, and, less commonly, massive. The total Fe content in them varies from 27 to 56%, averaging 40.5%.

The Innyaga area is located in the upper reaches of the Innyaga Creek, the left tributary of the Omolon River. It represents a narrow (2 km) block of the basement 8 km long among volcanics of the Kedon Complex, which is dated to the Middle–Late Devonian (Fig. 1) [3, 4]. The southern and southwestern parts of the area are marked by intrusive bodies of Early Carboniferous quartz diorites and Cretaceous rhyolites. The metamorphites developed in this area are intensely dislocated into steep submeridional folds.

The ore-hosting sequence is composed of gneisses, ferruginous quartzites, quartzite gneisses, crystalline schists, and amphibolites, which are granitized to a variable extent with the formation of migmatite granites. The rocks are universally intruded by Late Proterozoic metagabbro sills and dikes of the Strelka Complex. The ore lodes are represented by five conformable stratiform and lenticular bodies of ferruginous quartzites up to 10–50 m thick. Their length ranges from 200 to 1400 m. The ferruginous quartzites are characterized by massive and lenticular–banded structures, being composed of medium-grained magnetite, quartz, and amphibole. The total Fe content in the ores varies from 20 to 41%, averaging 38.5%.

The Magnetitovyi area is defined on the left side of the Omolon River in the Innyaga and Russkaya river interfluvium (Fig. 1). In this area, the ore-hosting sequence is composed of migmatized amphibolites, gneisses, quartzite gneisses, and quartzites dipping in the monoclonal manner in the westerly direction at angles of 60°–85°. The rocks are intruded by many metabasite sills and dikes of the Strelka Complex. Metamorphites are overlain by volcanics of the Kedon Complex in the west and bounded by Early Paleozoic granites of the Koargychan Massif in the south. The area comprises five bodies of ferruginous quartzites 15–80 m thick and 300–800 m long. The ores are characterized by diverse structural patterns: massive, banded, lenticular–banded, plaiting, densely disseminated, spotty, and irregularly disseminated. They are composed of magnetite (15–40%), quartz (15–40%), amphibole (5–25%), chlorite (1–10%), epidote, and apatite (1%). The Fe content in them is as high as 39.9% on average.

The Alekseevskii area is located on the right side of the Nizhnii Koargychan River near its mouth (Fig. 1). The western and eastern parts of the area are composed of Late Archean pagogneisses (Nodla Complex) and Early Proterozoic granite gneisses (Verkhniy

Omolon Complex), respectively. They also include lenticular bodies of variably migmatized amphibolites. The rocks are characterized by a northeastern strike with southeastward dip at angles of 50°–75°. In the central part of the area, metamorphites are marked by a mineralization zone with isolated lenticular bodies of ferruginous quartzites 1–2 m thick and 20–30 m (rarely 50 m) long. The Fe content in them ranges from 32 to 38%. The mineralization intensity increases toward the center of the zone. The zone is 2100 m long and 500–750 m wide. Along the zone axis, metamorphites are intruded by a dike of Early Paleozoic syenites of the Anmandykan Complex, which gives way in the southwesterly direction to diorites. The dike is up to 200 m thick and approximately 3 km long. The diorites and syenites contain veinlets and lenticular bodies of amphibolized varieties with disseminated magnetite concentrated in the zone up to 30 m wide and approximately 300 m long. The total Fe content is 15–21%.

RESULTS AND DISCUSSION

Diagnostics of Magmatic Minerals

Dependence of magnetic susceptibility on temperature The analysis of the $k(T)$ curves available for the examined samples reveals that magnetite with the Curie temperature of approximately 580°C is the principal magnetic mineral. At the same time, these curves differ in their particular features (Fig. 2). The heating curves obtained for some samples exhibit bends in the 400–450°C area, which are thought to be related to cation-deficient magnetite (maghemite) (Figs. 2a, 2c, 2e, 2g). This mineral is resistant relative to heating, when it is transformed into hematite. The maghemite-to-hematite transformation temperature is highly variable (from 250 to 900°C) depending on admixtures, size and shape of grains, degree of oxidation, genesis, and heating rate [2, 17, 18]. In heating curves $J_s(T)$ and $k(T)$, this transformation is recorded as the J_s and k drop at approximately 400°C [20, 21, 23, 24], which is characteristic of the examined samples. After heating, the magnetic susceptibility, as well as the saturation magnetization values, decrease, since both the magnetic susceptibility and J_s of hematite are hundreds of times lower as compared with these parameters in magnetite and maghemite [26] and the cooling curves are located below the heating curves. Such curves are characteristic of ferruginous quartzites and other rock types (Figs. 2a, 2c, 2e, 2g). Heating in the air medium results in partial oxidation of the magnetite. Some samples were heated in the argon medium (Fig. 2b, 2g, 2h). Judging from the $k(T)$ curves, no oxidation of magnetite occurs under such conditions. All the cooling curves are located above the heating curves, reflecting the formation of magnetite, probably, after hematite. The presence of the latter is confirmed by optical methods. At the same time, it may also be determined by the transition of maghemite into

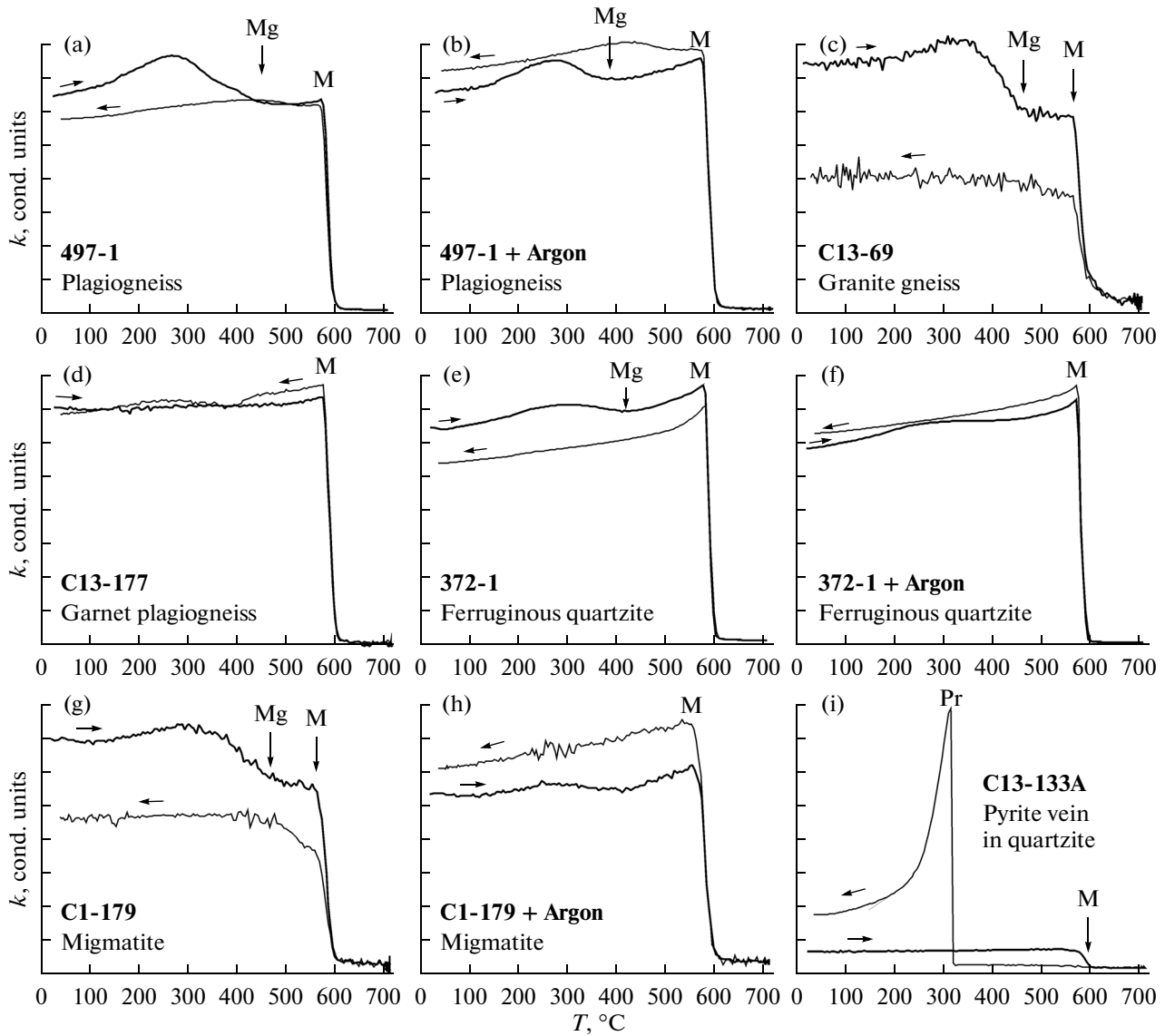


Fig. 2. Thermomagnetic curves. (M) magnetite; (Mg) maghemite; (Pr) pyrrhotite. Bold designates sample numbers, arrows indicate heating and cooling curves and Curie points (transition) of minerals.

magnetite, which is established, for example, for the ferruginous quartzites of the Kola Peninsula heated in a vacuum oven [1].

The heating and cooling curves obtained for the sample of garnet plagiogneiss are typical of magnetite, being practically reversible, which indicates stability of the magnetic minerals during heating (Fig. 2d). Sample C13-133 contains pyrite (Fig. 2i). The cooling curves $k(T)$ demonstrate the susceptibility increase at approximately 320°C, which corresponds to the Curie point of pyrrhotite, which results from the pyrite transformation into monoclonal pyrrhotite during heating [12, 27].

Dependence of saturation magnetization on temperature. Changes in saturation magnetization during

heating were studied for all of the samples from the examined rock collection. The curves $J_s(T)$ obtained for most samples are identical. The first-heating curves demonstrate the magnetization drop at the magnetite Curie temperature of approximately 580°C (Fig. 3).

The second-heating curves of many samples are located below their first-heating counterparts (Fig. 3). This is explained by the oxidation of magnetite and transformation of maghemite into hematite. Due to the high heating rates, the maghemite-to-hematite transition in curves $J_s(T)$ is vague, although it is distinct in the differential curves (omitted from the figures). Some second-heating curves are located above their first-heating counterparts, reflecting the appear-

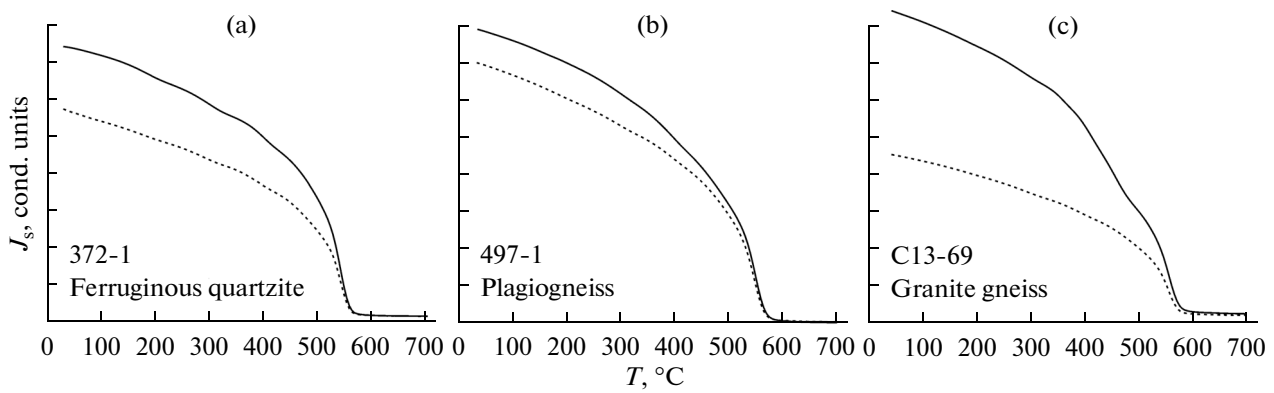


Fig. 3. $J_s(T)$ curves indicating that magnetite is the principal ferromagnetic mineral. The solid and dashed lines designate the first and second heating curves, respectively.

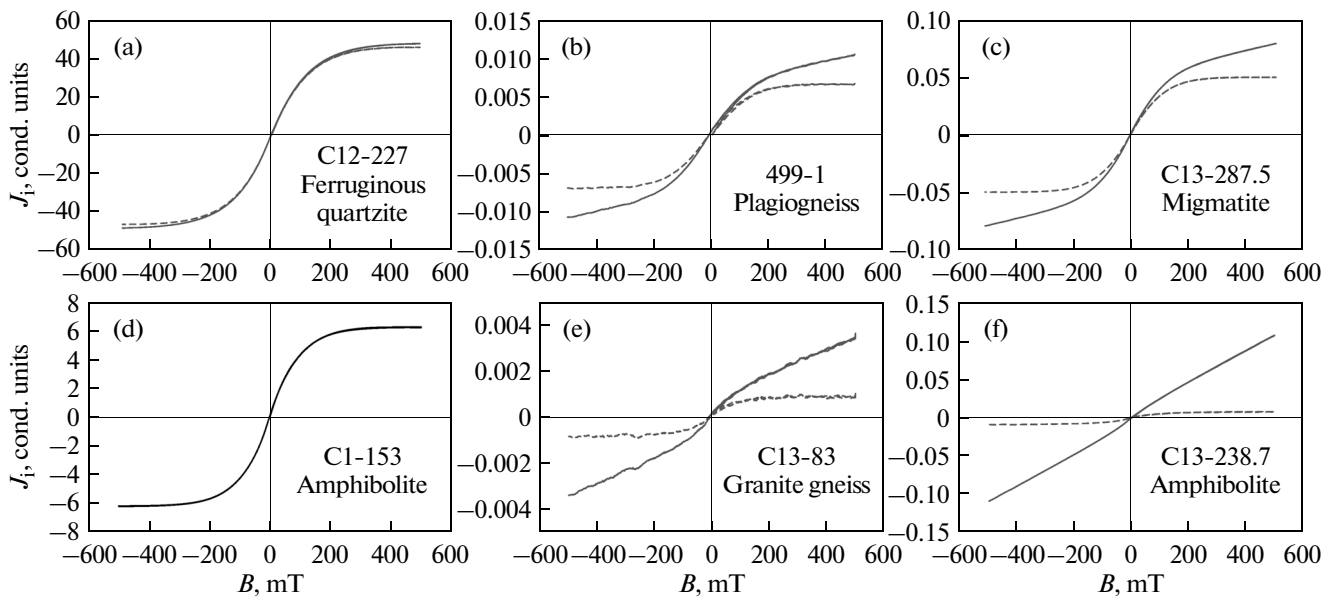


Fig. 4. Typical hysteresis loops of samples. Solid and dashed lines designate inductive magnetization uncorrected and corrected for the paramagnetic component, respectively.

ance of newly formed magnetite resulting from the transformations of paramagnetic Fe-bearing minerals. The curves obtained for single samples are repeatable, which is indicative of the stability of magnetic minerals during heating (omitted from the figures).

Hysteresis parameters. Figure 4 illustrates typical hysteresis loops. The paramagnetic component of inductive magnetization in most ferruginous quartzites is usually low, rarely exceeding 10%. In the samples of granite gneisses, garnet plagiogneiss, migmatites, plagiogneisses, and amphibolites, the paramagnetic component is frequently present in a more notable share, amounting to 90% (Figs. 4b, 4c, 4e, 4f).

Judging from the distribution of the J_{rs}/J_s and B_{cr}/B_c values in the Day diagram [16], the magnetic minerals of the amphibolites from the Innyaga area

and granite gneiss are characterized by the pseudosingle-domain structure, while the magnetic minerals in the plagiogneisses and migmatites are multidomain. The magnetic minerals from almost all the quartzites are multidomain (Fig. 5a).

It should be noted that multidomain particles are magnetically soft, being easily remagnetized by the present-day field. Stable remanent magnetization is usually determined by single- and pseudosingle-domain particles.

As expected, the ferruginous quartzites are characterized by maximum values of inductive magnetization, saturation magnetization, and remanent saturation magnetization (table).

Optical mineralogy. In ferruginous quartzites, the ore minerals form nest-shaped accumulations and

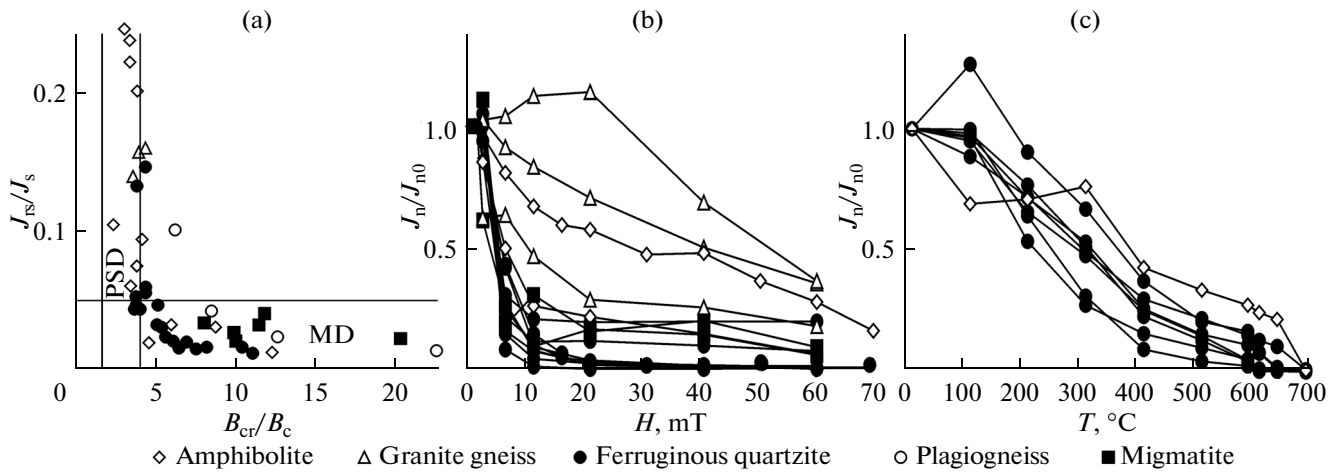


Fig. 5. The Day plot (a) and curves of rock demagnetization by the variable magnetic field (b) and temperature (c). (PSD) pseudo-single-domain structures; (MD) multidomain structures.

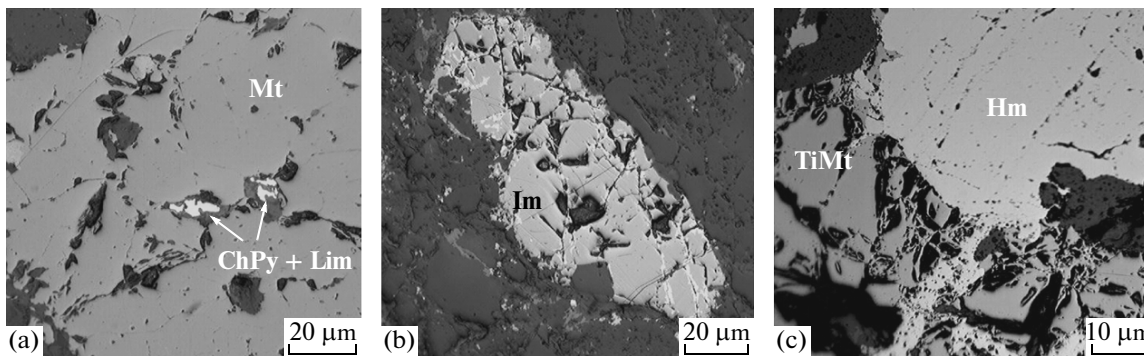


Fig. 6. Characteristic mineral interrelations in ores. (a) Sample 753-6c; (b) Sample 595-3; (c) Sample 1043-1c. (Mt) magnetite, (TiMt) titanomagnetite, (ChPy) chalcopyrite, (Hm) hematite, (Im) ilmenite, (Lim) limonite.

bands extended parallel to the metamorphic rock banding. These minerals are dominated by magnetite, which is frequently replaced along microfissures and in the marginal parts of accumulations by hematite and Fe hydroxide (Fig. 6).

Less common are the following minerals: low-Ti titanomagnetite: Fe (97.69–99.78%), Ti (1.40–1.55%); ilmenite: Fe (45.87–55.85%), Ti (47.54–56.30%); chalcopyrite: Fe (29.90–30.80%), Cu (31.71–34.14%), S (30.30–32.94%); pyrite: Fe (44.82–46.26%), S (50.82–52.59%).

NRM Stability

Two groups of samples are definable on the basis of the curves of NRM demagnetization by the variable magnetic field. The dominant group of samples (quartzites, migmatites) is characterized by a sharp magnetization drop in low magnetic fields. The median destructive field for them should be at least

5 mT. The magnetization (J_n) of the amphibolites, granite gneisses, and plagiogneisses is more stable (Fig. 5b). The ferruginous quartzites were largely used for stepwise thermal demagnetization. All the obtained curves are uniform, being characterized by a gradual magnetization decrease (Fig. 5c). After heating up to 600°C, most samples retain <1% of the initial magnetization values. In these samples, the magnetization is determined by magnetite. For some samples, the magnetization after heating to these temperatures retains 10–25% of its initial value. This magnetization component is determined by hematite. As was noted, hematite is not reflected in the $J_s(T)$ curves. Special investigations of a hematite–magnetite mixture with different proportions of these minerals revealed that hematite becomes reflected in the magnetic parameters only in situations when its proportion exceeds 95% [17].

Petrophysical rock properties

Area	N	Rock	$J_n, 10^{-3} \text{ A/m}$	$k, 10^{-3} \text{ SI}$	$J_{\text{IS}} \text{ Am}^2/\text{kg}$ av.	$J_s \text{ Am}^2/\text{kg}$ av.	J_{IS}/J_s av.	$\frac{B_{\text{ct}}/B_c}{\text{av.}}$	Q	$\rho, \text{ g/cm}$
Innyaga	2	Migmatite	1.50–2.77 (2.14)	0.04–0.05 (0.05)	0.00015	0.0033	0.04	9.05	0.84–1.70 (1.27)	2.45–2.50 (2.48)
	6	Amphibolite	792.00–7434.00 (2823.67)	6.84–58.14 (34.94)	0.35	1.63	0.23	3.48	0.75–4.32 (2.08)	2.42–2.72 (2.58)
	26	Ferruginous quartzite	22877– 1196362.00 (295147.69)	182–1588 (1046.15)	1.27	34.73	0.036	5.26	0.79–30.88 (7.19)	2.79–3.9 (3.38)
Verkhni Omolon	7	Amphibolite	3.57–28618.36 (4939.79)	0.84–177.30 (45.44)	0.11	1.60	0.074	4.32	0.11–4.06 (1.61)	2.80–3.67 (3.04)
	6	Migmatite	7.42–368.76 (120.10)	0.18–21.99 (6.39)	0.0042	0.134	0.03	13.42	0.001–1.86 (0.44)	2.61–2.68 (2.64)
	1	Andesite	336.70	17.72					0.48	2.96
	10	Granite gneiss	1.26–12656.00 (1769.65)	0.04–661.50 (71.67)	0.0034	0.179	0.15	4.91	0.15–12.18 (2.20)	2.50–3.71 (2.75)
	1	Garnet plagiogneiss	49.13	13.74	0.0014	0.206	0.007	20	0.09	3.01
Magnetitovyi	1	Quartzite sandstone	0.48	–0.005116	0.0001	0.0017	0.04	1.54	–2.36	2.64
	28	Ferruginous quartzite	11519.3–388278 (119739.07)	650.6–2388 (1394.37)	0.81	38.22	0.023	8.86	0.27–6.67 (2.11)	3.1–3.8 (3.53)
	6	Amphibolite	0.52–16701.00 (2890.76)	0.05–36.67 (8.74)	0.0052	0.122	0.044	15.90	0.09–11.45 (2.69)	2.62–3.04 (2.84)
	10	Plagiogneiss	0.35–1215.40 (152.93)	0.04–29.07 (5.19)					0.12–1.65 (0.52)	2.56–2.96 (2.71)
	2	Granite gneiss	1.10–15.54 (8.32)	0.14–2.65 (1.40)					0.15–0.20 (0.18)	2.57–2.59 (2.58)
Alekssevskii	1	Granite porphyry	2.54	0.32					0.20	2.531
	1	Rhyolite	2.36	0.03					1.86	2.53
	4	Plagiogneiss	64.94–2252.25 (652.73)	1.05–37.72 (12.23)	0.015	0.762	0.045	12.65	0.15–21.61 (5.89)	2.61–2.72 (2.66)
	1	Amphibolite	5684.09	6.58	0.087	0.94	0.093	4.3	21.68	3.00
	1	Migmatite	231.51	25.34	0.011	0.285	0.039	12.0	0.23	2.61

N number of samples.

Petrophysical Parameters

The Table presents the petrophysical parameters of the studied rocks. The maximum values of magnetic parameters are characteristic of the ferruginous quartzites from the Innyaga area, where J_n is as high as ranging from 22.8 to 1196 A/m and k averages 1046×10^{-3} SI. High values of magnetic parameters are also established for the amphibolites: J_n is 28.6 A/m and k is 45×10^{-3} SI. The magnetic parameters (J_n and k) of the plagiogneisses and granite gneisses are highly variable in wide limits. The migmatites, rhyolites, and dacites are submagnetic. The quartzite–sandstone sample is characterized by insignificant negative magnetic susceptibility. It is conceivable that the rock-forming minerals in this sample are represented by diamagnetic minerals, whereas the insignificant J_n value is determined by some admixture of magnetic minerals.

The Q factor value for all the studied rocks from the areas under consideration vary from <1 to >1 (table). Analysis of the Q factor distribution in the rocks revealed that the values of this parameter are controlled by the component composition of the natural remanent magnetization vector and the composition of the magnetic minerals.

The same rocks demonstrate different magnetic properties in different areas. These variations are determined by many factors: the NRM nature; the domain state of magnetic minerals; and the content of magnetite and products of its oxidation—maghemite, hematite, and Fe hydroxides [22].

Parameters of Sources of Magnetic Anomalies

Highly magnetic amphibolites and ferruginous quartzites may be responsible for magnetic anomalies.

Amphibolites are represented by samples taken from all areas. The samples from the Verkhni Omolon and Magnetitovyi areas demonstrate significant positive correlation between natural remanent magnetization and magnetic susceptibility: the correlation coefficients (r) are 0.94 and 0.95, respectively. At the same time, no correlation between J_n and density or between k and density for these areas is observable. For the samples from the Innyaga area, the coefficient of correlation between J_n and k is lower at 0.58. At the same time, they exhibit positive correlation between J_n and density ($r = 0.46$) and between k and density ($r = 0.87$). The petromagnetic properties of the amphibolite samples from this area are controlled by the domain state of the particles. They are characterized by the maximum B_c and B_{cr} values: 11.8–43.9 and 60.5–109.1 mT, respectively.

The J_{rs}/J_s and B_{cr}/B_c values (0.23 and 3.48 in average, respectively) imply a dominant role of pseudosingle-domain particles, while the samples from other areas are dominated by multidomain particles. The amphibolites are largely magnetized in accordance

with the present-day magnetic field. They are relatively stable and are resistant to remagnetization by the laboratory magnetic field. Judging from the demagnetization results, their magnetization is easily destroyed by the variable field, although the magnetization direction remains unchanged. The high NRM and magnetic susceptibility values provide grounds for the conclusion that these rocks may substantially contribute to the intensity of positive magnetic anomalies.

Ferruginous quartzites were studied in the Verkhni Omolon and Innyaga areas. They differ from each other in magnetic parameters. The samples from the Innyaga area are characterized by a positive correlation between J_n and k , between J_n and density, and between k and density (correlation coefficients 0.40, 0.50, and 0.56, respectively). The coefficient of correlation between J_n and k for the samples from the Verkhni Omolon area is 0.2. No correlation is found between J_n and density or between k and density. Almost all the quartzite samples are characterized by the multidomain structure, although the J_{rs}/J_s value is higher for the quartzites from the Innyaga area (0.034 on average) as compared with that for their counterparts from the Verkhni Omolon area. The B_{cr}/B_c value obtained for the samples from the Innyaga and Verkhni Omolon areas averages 5.3 and 8.6, respectively. Magnetization of the quartzites is mostly represented by the magnetically soft component. The variable magnetic field of 10 mT (100 Oe) destroys over 90% of the natural remanent magnetization. Microscopic investigations show that the magnetite ore also includes hematite, although its contribution to the natural remanent magnetization and magnetic susceptibility is insignificant. Our studies revealed no distinct correlation between the Fe_2O_3 content and magnetic susceptibility, which is likely explained by the different quantitative and qualitative proportions of the magnetic minerals.

The ferruginous quartzites are characterized by high values of magnetic susceptibility, which induces magnetization oriented along the present-day field. The quartzites also exhibit high values of natural remanent magnetization with positive and negative inclinations.

The NRM values obtained for the ferruginous quartzites from the Innyaga area are higher as compared to this parameter in their counterparts from the Verkhni Omolon area. In contrast, the magnetic susceptibility is higher in the Verkhni Omolon area than in the Innyaga area.

The Q factor of the rocks in the Innyaga area is characterized by higher values and, thus, their NRM may contribute greatly to the anomalous field.

In the Verkhni Omolon area, the Q factor demonstrates lower values, with the gradient of the anomalous zones being slightly smoothed and provided by inductive magnetization of rocks.

The superposition of inductive and natural remanent magnetization should determine both the direction and intensity of the magnetic anomalies induced by these rocks. The vertical alternation of normally and reversely magnetized quartzites makes determination of the sum NRM direction difficult. It should be noted that natural remanent magnetization is more readily recognizable by the methods of ground magnetic survey since it may influence intensity of anomalies at the surface due to the different polarity of the J_n vector, while induced magnetization is more easily detected by aeromagnetic and satellite-based surveying [8, 10, 15].

CONCLUSIONS

(1) Study of the petromagnetic properties of the rocks in the region under consideration has revealed their high diversity.

Anomalously high values of natural remanent magnetization and magnetic susceptibility are characteristic of the ferruginous quartzites and, to a lesser extent, amphibolites, while the migmatites, plagiogneisses, granite gneisses, and Paleozoic volcanics exhibit substantially lower values of these parameters.

(2) The magnetic minerals in the examined rocks are largely represented by magnetite with the multidomain and, less commonly, pseudosingle-domain structure accompanied by subordinate hematite and maghemite.

(3) The amphibolites and ferruginous quartzites may serve as sources for magnetic anomalies of different directions and intensities. The former are magnetized in accordance with the present-day magnetic field, while the latter demonstrate both normal and reverse polarities.

ACKNOWLEDGMENTS

This work was partially supported by the Far East Branch of the Russian Academy of Sciences (grant no. 12-III-A-08-191).

REFERENCES

1. S. S. Absalyamov and V. N. Khaibullin, "Magnetic properties of BIFs subjected to the pressure-induced shearing," *Fiz. Zemli*, No. 3, 77–80 (2002).
2. B. V. Burov, D. K. Nurgaliev, and P. G. Yasonov, *Paleomagnetic Analysis*, Ed. by V. P. Boronin (Izd-vo KGU, Kazan, 1986) [in Russian].
3. M. Kh. Gagiev, *Middle Paleozooids of Northeast Asia* (SVNTs DVO RAN, Magadan, 1996) [in Russian].
4. M. Kh. Gagiev, V. S. Shul'gina, and A. M. Gagieva, "New data on the Paleozoic stratigraphy of the Southern Omolon Massif," in *Essays on Stratigraphy of Northeast Asia* (SVKNII DVO RAN, Magadan, 2000), pp. 57–97 [in Russian].
5. M. L. Gel'man, V. A. Titov, and A. P. Fadeev, "Omolon Iron Ore Province," *Dokl. Akad. Nauk SSSR* **218** (2), 419–422 (1974).
6. M. L. Gel'man and A. P. Fadeev, "Iron," in *The USSR Geology. Vol. 30. Northeast USSR (Magadan Krai and Okhotsk District). Mineral Resources*, Ed. by P. V. Babkin and M. E. Gorodinsky (Nedra, Moscow, 1983), pp. 34–44 [in Russian].
7. N. A. Goryachev, S. M. Rodionov, V. V. Ratkin, V. I. Shpikerman, R. A. Eremin, A. A. Sidorov, and V. V. Naumova, "Metallogenic belts and ore districts of East Russia," in *Geodynamics, Magmatism, and Metallogeny of East Russia*, Ed. by A. I. Khanchuk (Dal'nauka, Vladivostok, 2006), Vol. 2, pp. 779–854 [in Russian].
8. A. I. Didenko, A. Yu. Peskov, V. A. Gur'yanov, A. N. Perestoronin, and A. V. Kosynkin, "Paleomagnetism of the Ulkan Trough (southeastern Siberian Craton)," *Russ. J. Pac. Geol.* **7** (1), 26–45 (2013).
9. I. L. Zhulanova, *Earth's Crust of Northeast Asia in the Precambrian and Phanerozoic* (Nauka, Moscow, 1990) [in Russian].
10. E. G. Ivolga, "Petrophysical studies in developing the geophysical models of ore district: evidence from the Voznesensky ore district, Primorye," *Tikhookean Geol.* **29** (4), 91–113 (2010).
11. *Magnetic Survey. A Handbook of Geophysist*, Ed. by V. E. Nikitskii and Yu. S. Glebovskii (Nedra, Moscow, 1980) [in Russian].
12. P. S. Minyuk, E. E. Tyukova, T. V. Subbotnikova, A. Yu. Kazanskii, and A. P. Fedotov, "Thermal magnetic susceptibility data on natural iron sulfides of northeastern Russia," *Tikhookean Geol.* **54** (4), 601–614 (2013).
13. N. I. Tret'yakova and M. I. Parfenov, "New data on the geological structure of the Verkhneomolonskoe iron ore deposit (Magadan region)," in *Geology, Geography, and Biological Diversity and Resources of Northeast Russia: Proceedings of the Far East Regional Conference on 100th Anniversary of A. P. Vas'kovskii, Magadan, Russia, 2011* (SVNTs DVO RAN, Magadan, 2011), p. 58 [in Russian].
14. A. P. Fadeev, "Iron ore occurrences of the South Omolon District," *Kolyma*, No. 6, 41–43 (1975).
15. L. M. Alva-Valdivia and H. López-Loera, "A review of iron oxide transformations, rock magnetism and interpretation of magnetic anomalies: El Morro Mine (Brazil), a case study," *Geofis. Int.* **50** (3), 341–362 (2011).
16. R. Day, M. Fuller, and V. A. Schmidt, "Hysteresis properties of titanomagnetites: grain-size and compositional dependence," *Phys. Earth Planet. Int.* **13**, 260–267 (1977).
17. C. B. De Boer and M. J. Dekkers, "Unusual thermomagnetic behaviour of haematites: neoformation of a highly magnetic spinel phase on heating in air," *Geophys. J. Int.* **144**, 481–494 (2001).
18. D. J. Dunlop and Ö. Özdemir, *Rock Magnetism: Fundamental and Frontiers* (Univ. Press, Cambridge, 1997).
19. U. Frank and N. R. Nowaczyk, "Mineral magnetic properties of artificial samples systematically mixed from haematite and magnetite," *Geophys. J. Int.* **175**, 449–461 (2008).

20. M. J. Hill, Y. Pan, and C. J. Daviesa, "An assessment of the reliability of palaeointensity results obtained from the Cretaceous aged Suhongtu section, Inner Mongolia, China," *Phys. Earth Planet. Int.* **169**, 76–88 (2008).
21. S. Hu, S. R. Goddu, E. Appel, and K. Verosub, "Fine-tuning of age integrating magnetostratigraphy, radio-carbon dating, and carbonate cyclicity: example of lacustrine sediments from Heqing Basin (Yunnan, China) covering the past 1 Myr," *J. Asian Earth Sci.* **30**, 423–432 (2007).
22. M. R. Hudson, V. J. S. Grauch, and S. A. Minor, "Rock magnetic characterization of faulted sediments with associated magnetic anomalies in the Albuquerque Basin, Rio Grande Rift, New Mexico," *Geol. Soc. Am. Bull.* **120** (5–6), 641–658 (2008).
23. N. Jordanova, D. Jordanova, and P. Petrov, "Magnetic imprints of pedogenesis in planosols and Stagnic Alison from Bulgaria," *Geoderma* **160**, 477–489 (2011).
24. D. Krasa and E. Herrero-Bervera, "Alternation induced changes of magnetic fabric as exemplified by dykes of the Koolau Volcanic Range," *Earth Planet. Sci. Lett.* **240**, 445–453 (2005).
25. W. J. Noklenberg, T. D. West, K. M. Dawson, et al., "Summary terrane, mineral deposit and metallogenic belt maps of the Russian Far East, Alaska and the Canadian Cordillera," U.S. Geol. Surv. Open. File Rept., No. 98-136, (1998).
26. C. Peters and M. J. Dekkers, "Selected room temperature magnetic parameters as a function of mineralogy, concentration and grain size," *Phys. Chem. Earth* **28**, 659–667 (2003).
27. L. Wang, Y. Pan, J. Li, and H. Qin, "Magnetic properties related to thermal treatment of pyrite," *Sci. China. Ser. D: Earth Sci.* **51** (8), 1144–1153 (2008).

Recommended for publishing by A.N. Didenko

Translated by I. Basov